Polymer Bulletin 49, 69-76 (2002)

Polymer Bulletin


# Structure and thermal properties of compatibilized PET/expandable fluorine mica nanocomposites

**C.Saujanya, Y.Imai (✉), H.Tateyama**

Institute for Structural and Engineering Materials, National Institute of Advanced Industrial Science & Technology (AIST), 807-1, Shuku-machi, Tosu, Saga 841-0052, Japan,
e-mail: y-imai@aist.go.jp, Fax: +81-942-81-3693

Received: 17 May 2002 / Accepted: 12 July 2002

## Summary

A series of PET/expandable fluorine mica (ME) nanocomposites with different proportions of compatibilizer, 10-[3,5-*bis*(methoxycarbonyl)phenoxy]decyltriphenylphosphonium bromide (IP10TP) were prepared by in situ polymerization process. The crystallite size, nucleation and the effect of content of compatibilizer on the dispersibility of ME in PET matrix were investigated by XRD and DSC techniques. The XRD results showed a decrease in the crystallite size of ME giving rise to partially exfoliated structure and the crystallite size of PET reduced considerably as compared to pure PET at low content of IP10TP. The DSC results revealed a dramatic increase in crystallization temperature ($T_c$) and also showed enhancement in glass transition ($T_g$) and melting point ($T_m$) at low content of IP10TP. These various findings have been explained based on the miscibility of IP10TP/ME with PET.

## Introduction

Preparation of fully exfoliated, homogeneously dispersed clay nanocomposites in various polymer matrices is the subject of considerable interest among the various groups of researchers due to their significant performance improvements over their base polymers, which have been well noted [1-4].
Recently, introduction of an organic compatibilizer between polymer and clay has provided a new strategy to prepare dispersed clay nanocomposites. For example exfoliation of polypropylene (PP) [5,6] and polyethylene (PE) [7] nanocomposites could be accomplished by maleic anhydride modified PP & PE. In case of polystyrene (PS) nanocomposites [8], exfoliation was attained by the use of poly(styrene-co-oxazoline) copolymers as a compatibilizer and in case of poly(styrene-co-acrylonitrile) nanocomposites [9], poly(ε-caprolactone) facilitated good dispersion of clay. These polymer/clay hybrids were prepared by melt compounding technique. However, Mülhaupt and his coworkers [10] have reported that exfoliation of clay nanocomposites achieved by using melt compounding technique was not as effective

as in the case of in situ polymerization process. So far, the compatibilizing agents have been investigated in polymers such as PP, PE, PS, etc. Very few reports [11,12] have appeared for poly(ethylene terephthalate) (PET) nanocomposites using a compatibilizer. It should be noted that PET nanocomposites are commercially important for packaging, beverage and gas barrier applications. Recently, we have published the synthesis of PET/ME nanocomposites using a novel reactive compatibilizer, 10-[3,5-*bis*(methoxycarbonyl)phenoxy]decyltriphenylphosphonium bromide (IP10TP) by in situ polymerization process [13]. The above reactive compatibilizer was chosen for three main advantages: firstly its large size which can promote greater expansion of interlayer distance in the clay; secondly high reactivity can be achieved due to the presence of many functional groups at its periphery and thirdly the phosphonium cation of the compatibilizer forms a stable complex with clay at the polymerization temperature of PET.
In the present work, we have exploited the structure and thermal properties of PET/ME nanocomposites with different proportions of compatibilizer (IP10TP) by using XRD and DSC techniques. Further, the results obtained have been compared with PET/ME without IP10TP and pure PET.

## Experimental

Nanocomposites of PET/ME with a novel reactive compatibilizer (IP10TP) were prepared in three steps:
The first step consisted of preparation of compatibilizer, IP10TP; the synthetic route was first reported by us which has been described in our previous paper [13].
In the second step, the intercalation of IP10TP into ME with various proportions of IP10TP ranging from 0.2 to 1.2 mmole/g-ME was accomplished by cation exchange reaction. It should be noted that the two dimensional size of ME was about 6 μm and the cation exchange capacity of ME was 1.2 mmole/g.
The third step comprised of polymerization of *bis*(2-hydroxyethyl) terephthalate (BHET) in the presence of IP10TP/ME intercalation compounds using $Sb_2O_3$ catalyst at 275 °C under vacuum (< 0.1 Torr) thus giving rise to PET/IP10TP/ME nanocomposites. Here the content of ME with respect to BHET was held constant i.e 4 wt %. The complete procedure of synthesis has been explained in our previous paper [13].
The structure, crystallite size and the thermal properties of these nanocomposites were investigated by XRD and DSC techniques. The XRD patterns were obtained by using a Philips X-ray diffractometer (X´ Pert MPD ) equipped with Cu Kα radiation (λ = 1.542 Å) at a scan rate of 0.05 °/s. The DSC analysis was performed on a Rigaku (DSC8230D model) at a heating or cooling rate of 10 °C/min under $N_2$ atmosphere. The temperature range was from RT to 290 °C. The results obtained have been compared with uncompatibilized composite i.e PET/ME without IP10TP and pure PET synthesized in the same way as explained above.

## Results and discussion

Figure 1 depicts the WAXD scans for compatibilized nanocomposites represented by the curves C to H with decreasing content of IP10TP from 1.2 to 0.2 mmole/g-ME.

While curve B corresponds to PET/ME without IP10TP and curve A that of pure PET. Two key features can be observed in this graph. Firstly, a pronounced shift in the d-spacing from 0.96 nm which is the characteristic peak of ME to 1.96 nm for compatibilized nanocomposites clearly shows the evidence of more intercalation of PET chains in the galleries of mica platelets as compared to a slight shift of d-spacing from 0.96 nm to 1.25 nm for uncompatibilized composite (curve B). The curves C–G show the intercalated (ordered structure) and the curve H shows a partially exfoliated structure (disordered) with broad peak due to loss of peak intensity. Secondly, with decrease in the content of IP10TP from 1.2 to 0.2 mmole/g-ME, the intensity of PET peaks broaden considerably (as compared to pure PET) thus suggesting a reduction in the crystallite size of PET in the case of compatibilized nanocomposites as compared to uncompatibilized one.

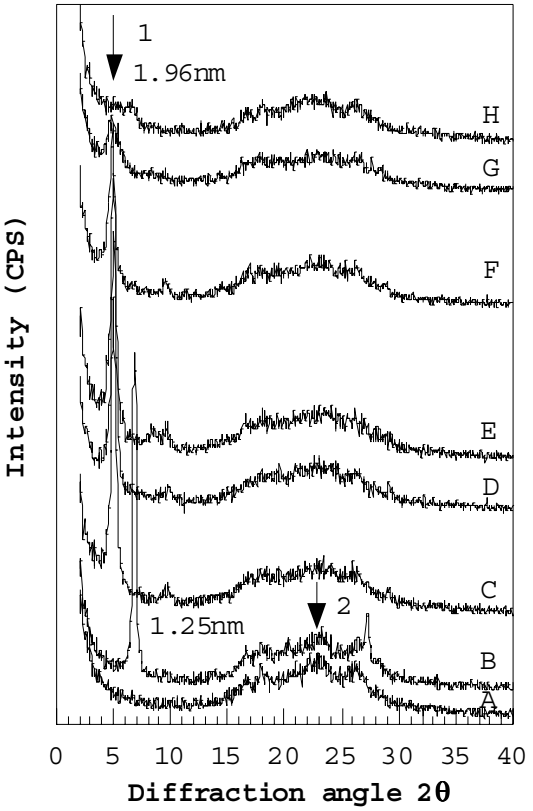


**Figure 1**. WAXD scans for compatibilized PET/ME nanocomposites with decreasing content of IP10TP from 1.2 to 0.2 mmole/g represented by the curves C–H while curve B corresponds to PET/ME without IP10TP and curve A that of pure PET.

The crystallite size was estimated from the full width at half maxima for the ME peak (marked as arrow 1) and for the PET peak (at $2\theta = 22.74^{\circ}$, marked as arrow 2) using Scherrer's formula [14,15]. The results are summarized in the Table 1. It can be noted that pure PET shows an average crystallite size of 9.7 nm whereas the compatibilized PET shows lowering of crystallite size and it reduces to 3.7 nm at low content (0.2 mmole/g-ME) of IP10TP. Similarly, the crystallite size of ME reduces to 8 nm at 0.2 mmole/g-ME of IP10TP as compared to 45 nm for the uncompatibilized one. The existence of reduction in the crystallite sizes of both ME and PET at low content of IP10TP confirms that there is a good miscibility between PET, IP10TP and ME leading to partially exfoliated structure of ME in the PET matrix.

**Table 1**. Crystallite sizes of ME and PET for compatibilized PET nanocomposites

| Composition | Crystallite size (L) in nm[a] | |
|---|---|---|
| | ME | PET |
| Pure PET | | 9.7 |
| PET/ME without IP10TP | 45 | 8.0 |
| PET/ME with IP10TP (1.2 mmole/g -ME) | 38 | 5.2 |
| PET/ME with IP10TP (1.0 mmole/g -ME) | 30 | 5.1 |
| PET/ME with IP10TP (0.8 mmole/g-ME) | 26 | 4.2 |
| PET/ME with IP10TP (0.6 mmole/g-ME) | 23 | 4.1 |
| PET/ME with IP10TP (0.4 mmole/g-ME) | 12 | 4.1 |
| PET/ME with IP10TP (0.2 mmole/g-ME) | 8 | 3.7 |

[a] Determined from Scherrer's formula.

The most striking feature of the present investigation can be observed in Fig. 2 which shows the graph of crystallization temperature ($T_c$) and melting point ($T_m$) of PET/ME nanocomposites as a function of IP10TP. There is a dramatic increase in $T_c$ for compatibilized nanocomposites as compared to uncompatibilized one and pure PET. This is also apparent from the cooling curves of DSC presented in Fig. 3 where the exothermic peak for compatibilized nanocomposite (curve C) becomes narrower and shifts to a higher temperature as compared to uncompatibilized composite (curve B) and pure PET (curve A). The $T_c$ increases by almost 12 $^{\circ}$C at low content (0.2 mmole/g-ME) of IP10TP than pure PET (207 $^{\circ}$C) and then shows a decrease with further increase in the content of IP10TP to 1.2 mmole/g-ME. It can be observed that PET/ME without IP10TP shows a value of $T_c$ of 212.7 $^{\circ}$C which is higher than $T_c$ of pure PET. From these findings it can be concluded that ME has a strong heterophase nucleation effect on PET. Although ME without IP10TP nucleates PET, stronger nucleation efficiency of PET can be observed for compatibilized nanocomposites especially at 0.2 mmole/g-ME of IP10TP due to the reduced size of ME crystallites which offer enormous surface area and hence gives rise to higher crystallization temperature of PET during nucleation. The melting point ($T_m$) of compatibilized nanocomposites also show enhancement at low content (0.2mmole/g-ME) of IP10TP as compared to uncompatibilized one which can be attributed to stronger interfacial interaction between ME and PET matrix.

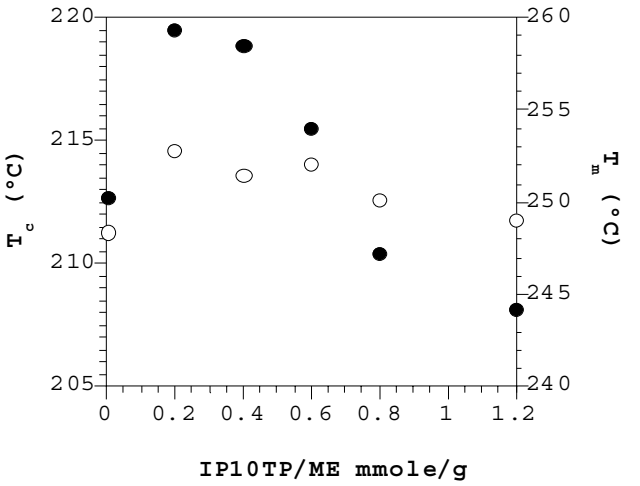


**Figure 2**. Crystallization temperature ($T_c$) and melting temperature ($T_m$) of PET/ME nanocomposites with increasing content of IP10TP. (● → $T_c$ , ○ → $T_m$ )

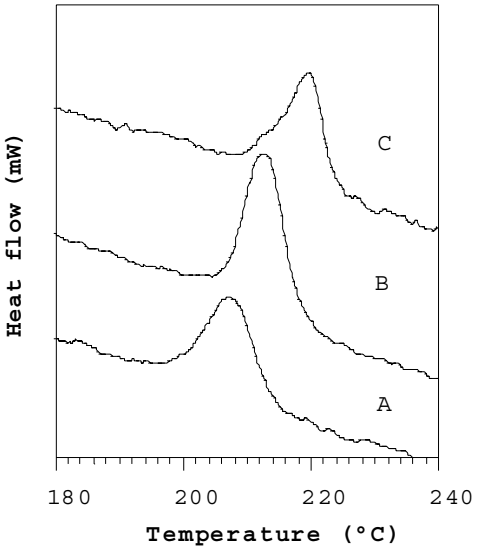


**Figure 3.** Cooling curves of DSC: A = pure PET, B= PET/ME and C= PET/ME with IP10TP (0.2 mmole/g-ME)

Figure 4 shows the graph of glass transition ($T_g$) of these nanocomposites as a function of IP10TP. It can be seen that $T_g$ is found to decrease with increase in the content of IP10TP whereas for PET/ME without IP10TP, the $T_g$ remains unchanged and shows a value similar to pure PET (72.5 °C). The increase of $T_g$ for compatibilized nanocomposites especially at low content of IP10TP can be ascribed to the restricted segmental motions near the PET-ME interfaces.

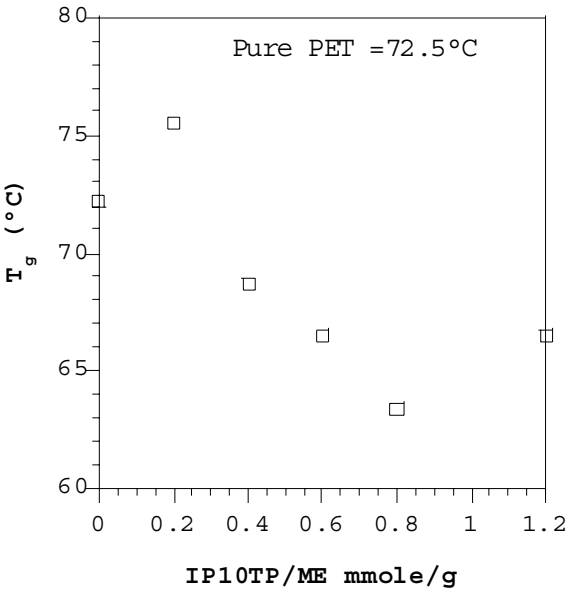


**Figure 4**. Glass transition temperature ($T_g$) for PET/ME nanocomposites with increasing content of IP10TP

Table 2 represents the percentage crystallinity ($C_i$) of the PET/IP10TP/ME nanocomposites determined from DSC measurement. The $C_i$ was calculated from the enthalpy value (ΔH) obtained from the melting endotherms of the nanocomposites and the enthalpy value for a theoretically 100% crystalline PET taken from the literature

**Table 2.** Percentage crystallinity values ($C_i$) for PET/IP10TP/ME nanocomposites

| Composition | Crystallinity ($C_i$) % |
|---|---|
| Pure PET | 23 |
| PET/ME without IP10TP | 22 |
| PET/ME with IP10TP (1.2 mmole/g-ME) | 23 |
| PET/ME with IP10TP (0.8 mmole/g -ME) | 21 |
| PET/ME with IP10TP (0.6 mmole/g -ME) | 22 |
| PET/ME with IP10TP (0.4 mmole/g -ME) | 20 |
| PET/ME with IP10TP (0.2 mmole/g -ME) | 21 |

[16]. The crystallinity values remain more or less unaffected for the compatibilized nanocomposites for the same content of ME as compared to the uncompatibilized composite and pure PET.

## Conclusions

We have demonstrated the structure and thermal properties of PET/ME nanocomposites with IP10TP as a novel reactive compatibilizer by varying the content of IP10TP from 0.2 to 1.2 mmole/g-ME. The XRD analysis revealed a considerable reduction in the crystallite sizes of both ME as well as PET at low content of IP10TP thus suggesting that ME platelets could be partially exfoliated in PET matrix. These exfoliated ME platelets played a strong nucleating role by exhibiting a drastic increase in the crystallization temperature $T_c$ as compared to uncompatibilized composite. Further significant increase in $T_g$ and $T_m$ were also seen. However, their crystallinity values remained unaffected compared to PET/ME without IP10TP and pure PET.
Thus, from the present study, it can be concluded that the compatibilizer, IP10TP plays an important role by promoting sufficient miscibility between polymer and clay giving rise to formation of exfoliated structure.

## References


1. Giannelis EP, Krishnamoorthi R, Manias E (1999) Adv Polym Sci 138: 107
2. LeBaron PC, Wang Z, Pinnavaia TJ (1999) Appl Clay Sci 15:11
3. Wang Z, Lan T, Pinnavaia TJ (1996) Chem Mater 8:2200
4. Smoug D (1998) Mod Plast 2:28
5. Hasegawa N, Kawasumi M, Kato M, Usuki A, Okada A (1998) J Appl Polym Sci 67:87
6. Kawasumi M, Hasegawa N, Kato M, Usuki A, Okada A (1997) Macromolecules 30:6333
7. Wang KH, Choi MH, Choi YS, Chung IJ (2001) Polymer 42(24):9819
8. Hasegawa N, Okaoto H, Kawasumi M, Usuki A (1999) J Appl Polym Sci 74:3359
9. Kim SW, Jo WH, Lee MS, Ko MB, Jho JY (2001) Polymer 42:9837
10. Heinemann J, Reichert P, Thomann R, Mülhaupt R (1999) Macromol Rapid Commun 20:423
11. Tsai TY, Hwang CL and Lee SY (2000) SPE-ANTEC Proc 248 :2412
12. Pinnavaia TJ and Beall GW (2001) Polymer-Clay Nanocomposites, Chap 9, p173, Wiley Series in Polymer Science
13. Imai Y, Nishimura S, Abe E, Tateyama H, Abiko A, Yamaguchi A, Aoyama T and Taguchi H (2002) Chem Mater 14:477
14. Hindeleh AM, Johnson DJ (1978) Polymer 19:29
15. Alexander LE (1969) X-ray Diffraction Methods in Polymer Science. New York. Wiley, p 335
16. Vilanova PC, Ribas SM, Martin GG (1985) Polymer 26:423
17. Roberts RC (1969) Polymer 10:113